Journal of Computer Assisted Tomography
26(6):894–901

Age-Dependent Change in Metabolic Response to Photic Stimulation of the Primary Visual Cortex in Infants: Functional Magnetic Resonance Imaging Study

Satoshi Muramoto, Hiroki Yamada, Norihiro Sadato, Hirohiko Kimura, Yukuo Konishi, Kouki Kimura, Masato Tanaka, Takanori Kochiyama, Yoshiharu Yonekura, and Harumi Ito

Abstract: The blood oxygen level-dependent (BOLD) response to photic stimulation in the primary visual cortex (V1) reverses from positive to negative around 8 weeks of age. This phenomenon may be caused by increased oxygen consumption during stimulation as the result of a rapid increase of synaptic density at this age. To test this hypothesis, we applied existing mathematic models of BOLD signals to the experimental data from infants. When the stimulus-related increments of cerebral blood flow and cerebral blood volume were fixed at 60% and 20%, respectively, the mean estimated increment of the cerebral metabolic rate of oxygen of the V1 in the elder infant group (57.1% ± 8.8%) was twice as large as that in the younger infant group (32.2% ± 4.7%), which corresponds to the reported difference in synaptic density. The present data confirmed that a change in oxygen consumption could explain a transition from a positive to a negative BOLD response. **Index Terms:** Infant brain—Functional MRI—Visual stimulation—BOLD model—Neural development—Cerebral metabolism.

The development of functional magnetic resonance imaging (fMRI) has enabled us to visualize human brain activity. Based on the assumption that energy-dependent changes in neuronal activity and cerebral blood flow (CBF) are coupled (1), fMRI studies have been successfully conducted during the performance of various tasks in human adult and animal studies. Magnetic resonance (MR) signal changes have been shown to be closely correlated spatially and temporally with CBF change (2–7). Unlike positron emission tomography, however, the relation between the MR signal change and CBF change is not straightforward.

Most fMRI techniques adopt blood oxygenation level-dependent (BOLD) signal change (8–11). The origin of BOLD signal change is related to the fact that deoxyhemoglobin is paramagnetic (12). Changes in the local deoxyhemoglobin concentration alter the magnetic susceptibility of blood. A difference in susceptibility between blood and the surrounding extravascular space generates microscopic magnetic field gradients in the vicinity of the blood vessels, which leads to intravoxel dephasing, resulting in a small loss of signal in MR images acquired with pulse sequences sensitive to field variations such as gradient-recalled echoes with long echo times (13). With neuronal activation, oxygen delivery, CBF, and cerebral blood volume (CBV) increase (11). Because CBF (and oxygen delivery) changes exceed CBV change two- to fourfold and the cerebral metabolic rate of oxygen ($CMRO_2$) increases only slightly (14,15), total deoxyhemoglobin decreases; hence, less intravoxel dephasing and increased MR signal occur (11,16). In summary, the reduction of the oxygen extraction fraction (OEF) accompanied by regional CBF increase is critical for an increase in the MR signal in the brain during neural stimulation (13). Hence, BOLD signal change may reflect change in oxygen metabolism.

Quantitative approaches to combine the physiologic parameters such as $CMRO_2$, CBF, and CBV have been reported by Buxton et al. (17). Because the task-related

Department of Radiology (S. Muramoto, H. Yamada, H. Kimura, M. Tanaka, and H. Ito), Department of Pediatrics (K. Kimura), and Biomedical Imaging Research Center (Y. Yonekura), Fukui Medical University, Fukui, Psychophysiology Section Department of Cerebral Research National Institute for Physiological Sciences, Aichi (N. Sadato), Department of Infants' Brain and Cognitive Development, Tokyo Women's Medical University, Tokyo (Y. Konishi), and Graduate School of Human and Environmental Studies, Kyoto University, Kyoto (T. Kochiyama), Japan. Address correspondence and reprint requests to Dr. S. Muramoto, Department of Radiology, Fukui Medical University, 23 Shimoaizuki, Matsuoka, Yoshida, Fukui, 910-1193, Japan. E-mail: muramoto@fmsrsa.fukui-med.ac.jp

BOLD signal change depends mainly on the change in the total deoxyhemoglobin content in an image voxel, BOLD signal change can be evaluated based on the change in total deoxyhemoglobin. In this model, the BOLD signal change relative to a baseline period was converted from the relative change in local deoxyhemoglobin concentration, which was derived from the changes in $CMRO_2$, CBF, and CBV normalized by ratio to a baseline period. The proposed models based on the measured data in the human adult brain and animals explained the findings of normal adult fMRI signals.

Recently, photic stimulation was shown to cause negative BOLD signal change in the primary visual cortex (V1) of infants (18,19). The task-related BOLD signal reversed from positive to negative at 8 weeks of corrected age (19,20). At about this period, synaptic density (21,22) and the regional cerebral metabolic rate of glucose (23) in the human V1 increase rapidly. These findings indicate that the negative response is caused by an increase in oxygen consumption accompanied by neural development (18,19). If the synaptic density number were doubled, the task-related energy consumption would be doubled, because most glucose consumption occurs at the synapse (1).

To test this hypothesis, we applied a mathematic model for BOLD signal change based on human adult and animal experiments (17) to infant fMRI data. The simulations showed that the positive-to-negative conversion in task-related BOLD signal change could be explained by a rapid increase in $CMRO_2$.

MATERIALS AND METHODS

Experimental Study: Infants

Subjects

From February 1997 to June 1998, we performed MRI and fMRI on the brains of 42 infants (23 male and 19 female), aged <1 year, whose perinatal risk factors warranted screening for possible brain damage. Patient data are summarized in Table 1. The indications for the MRI protocol are the screening of intracranial pathologic findings in patients with histories of birth asphyxia, prematurity, and infantile respiratory distress. To confirm normality, we prospectively followed up all 42 subjects after the MRI examination to note whether they showed normal neurologic development. The follow-up lasted at least until the subject reached 1 year of age. From the 42 patients, we selected 20 subjects (10 male and 10 female) for whom the neurologic and MRI findings were normal during the follow-up period. Thirteen of these 20 subjects were involved in the study by Yamada et al. (20), and 5 were included in the study by Morita et al. (24). At the time of fMRI examination they were aged <0 to 32 weeks, corrected for gestational age at birth. According to previous studies (20,24), they were divided into two groups: younger (corrected age <8 weeks, n = 10) and elder (corrected age >8 weeks, n = 10). The Ethical Committee of Fukui Medical University approved the protocol, and written informed consent for

TABLE 1. *Summary of patient data and functional magnetic resonance imaging results*

Patient	Sex	Age at functional magnetic resonance imaging		Response pattern	Maximum *z* score	History
		Corrected[a]	Chronologic			
1	m	0	12	p[b]	5.40	Asp (5)
2	m	0	9	p	4.52	Prematurity
3	f	2	2	p	4.59	Low birth weight
4	m	4	10	p	6.69	IRDS
5	m	6	17	p	6.48	IRDS
6	m	6	10	p	6.70	IUGR
7	f	6	17	p	5.25	IRDS
8	f	7	8	p	4.14	Acidosis
9	f	7	7	p	4.49	Asp (6)
10	m	7	16	p	4.18	Low birth weight
11	m	8	20	n[c]	5.18	Prematurity
12	f	8	8	n	5.22	Rule out of hydrocephalus
13	f	13	13	n	3.75	Hypothyroidism
14	f	13	18	n	6.16	Squint
15	f	17	26	n	5.06	Prematurity
16	f	18	23	n	4.53	IUGR
17	m	18	31	n	5.07	IRDS
18	m	29	33	n	4.99	IUGR
19	f	30	43	n	5.42	IRDS
20	m	32	32	n	4.16	Facial nerve palsy

[a] Corrected for gestational age at birth, calculated from the mother's last menstrual period.
[b] Positive.
[c] Negative.
m, male; f, female; Asp, birth asphyxia (Apgar score at 5 minutes); IRDS, infantile respiratory distress syndrome; IUGR, intrauterine growth retardation.

the study was obtained from the infants' parents before the examination.

MRI

All infants were sedated with 3 to 5 mg/kg of pentobarbital injected intravenously. The peripheral pulse rate and respiratory rate were monitored, and the infants were closely observed in the MRI unit. We confirmed that their eyes were closed via a mirror placed on the head coil during the study. Other than the constant gradient noise of echo planar imaging and the photic stimulation, sensory stimuli were minimized. A time course series of 102 volumes was acquired using T2*-weighted, gradient echo, echo planar imaging sequences using a 1.5-T MR imager (Signa; General Electric, Milwaukee, WI, U.S.A.). Each volume consisted of five slices with a slice thickness of 5 mm and a 1-mm gap approximately parallel to the calcarine fissure as determined by means of sagittal T2-weighted spin echo images as an anatomic guide. The time interval between two successive acquisitions of the same image was 3,000 milliseconds, the echo time was 50 milliseconds, and the flip angle was 90°. The field of view was 22 cm. The in-plane matrix size was 128 × 128 pixels, with a pixel dimension of 1.72 × 1.72 mm. The magnetic shim was optimized such that a true in-plane resolution of 1.72 × 1.72 mm could be realized. An initial baseline phase of rest for 30 seconds was followed by a photic stimulation phase for 30 seconds alternating with a rest phase, for a total of 10 phases per trial. Photic stimulation was performed with an 8-Hz flickering light projected onto the sedated infants' eyelids.

Image Analysis

The first two data points were discarded because of nonsteady magnetization, and the remaining 100 data points were analyzed. The significance of task-related signal change on each voxel was calculated by means of statistical parametric mapping (using software [SPM96] from the Wellcome Department of Cognitive Neurology, London, U.K.) implemented in MATLAB (Mathworks, Sherborn, MA, U.S.A.) (25,26). The images from each subject were realigned, with the first image used as a reference. The realigned fMRI data were filtered with a Gaussian kernel with full width at half maximum of 5, 5, and 10 mm for the x, y, and z axes, respectively. Finally, voxel-wise statistical analysis was performed by means of the general linear model (with temporal smoothing and autocorrelation over time) and statistical inference based on the spatial extent and maximum of threshold activation foci according to the theory of Gaussian fields. Significance was defined as $p < 0.05$ corrected for multiple comparisons. In an infant study, it is difficult to define the activation areas in the V1 based on an anatomic landmark (27,28). Therefore, we defined the region of interest in the V1 referring to the statistical parametric mapping. Signal intensity of the voxels, which showed maximum statistical confidence of the bilateral V1, was measured at each data point. In each subject, time intensity profiles of bilateral V1 were converted into percentage of signal time course with respect to the prestimulation signal level, which was obtained by averaging 10 time points in the first rest periods. The converted time courses of each region of interest on bilateral V1 of two sessions were averaged in each subject to generate one averaged time course of V1 per subject. Mean percentage of signal time course was calculated in each infant group.

Experimental Study: Adults

Subjects

As a control, we also performed fMRI in six normal adults (four male and two female), aged 23 to 31 years (25.5 ± 2.9 [mean ± SD]). This was to examine if the BOLD response of the younger children is similar to that of the adults for whom the model was constructed (17,29). The Ethical Committee of Fukui Medical University approved the protocol, and written informed consent for the study was obtained from the subjects before the examination.

MRI

A time course series of 42 volumes was acquired using T2*-weighted, gradient echo, echo planar imaging sequences with a 1.5-T MR imager (Signa). Each volume consisted of 12 slices with a slice thickness of 8 mm and a 1-mm gap covering the entire cerebral cortex. The time interval between two successive acquisitions of the same image was 3,000 milliseconds, the echo time was 50 milliseconds, and the flip angle was 90°. The field of view was 22 cm. The in-plane matrix size was 64 × 64 pixels, with a pixel dimension of 3.44 × 3.44 mm. The magnetic shim was optimized such that a true in-plane resolution of 3.44 × 3.44 mm could be realized. An initial baseline phase of rest for 30 seconds was followed by a photic stimulation phase for 30 seconds alternating with a rest phase, for a total of four phases per trial. Subjects' eyes were open during the study. Photic stimulation was performed with 8-Hz flickering (contrast reversing with a flicker rate of 8 Hz) checkerboard patterns projected onto a backlit projection screen just above the subject's foot. A mirror was positioned to allow the subject to view the image from the supine position.

Image Analysis

Data analysis of the adult study was identical to that of the infant study, except that the V1 was defined by an anatomic landmark depicted by T1-weighted images and

spatial smoothing was performed with a Gaussian kernel of 10 mm (full width at half maximum) in the x, y, and z axes.

Blood Oxygen Level-dependent Model

Theory

In a previous report, a model was devised to estimate changes in venous oxyhemoglobin concentrations based on changes in CBF, CBV, and $CMRO_2$ and was validated against fMRI data (17), in which all time course variables were normalized to the values at rest (17). Assuming that arterial hemoglobin is fully oxygenated and neglects capillary contribution and that all deoxyhemoglobin is in the venous compartment, the time course of total venous deoxyhemoglobin contents per voxel [Total Deoxy-Hb (t)] is expressed as

$$\text{Total Deoxy-Hb (t)} = \text{Deoxy-Hb Concentration (t)} \times \text{VBV (t)}, \quad (1)$$

where VBV is venous blood volume (17,29,30). Assuming that extracted oxygen from vascular space is consumed instantaneously (17), OEF can be defined as

$$\text{OEF (t)} = CMRO_2\text{ (t)}/[\text{CBF (t)} \times \text{Ca}], \quad (2)$$

where Ca is arterial oxygen concentration. One oxyhemoglobin is attached to four oxygen molecules. Assuming that all oxygen molecules are attached to hemoglobin, the intravascular concentration of deoxyhemoglobin is expressed as

$$\begin{aligned}&\text{Deoxy-Hb Concentration (t)}\\ &= \text{Oxy-Hb Concentration} \times \text{OEF (t)}\\ &= [\text{Ca}/4] \times \text{OEF (t)}\\ &= CMRO_2\text{ (t)}/[4 \times \text{CBF (t)}]\end{aligned}$$

Hence

$$\begin{aligned}&\text{Total Deoxy-Hb (t)}\\ &= CMRO_2\text{ (t)} \times \text{VBV (t)}/[4 \times \text{CBF (t)}] \quad (3)\end{aligned}$$

Temporal Response of Cerebral Metabolic Rate of Oxygen, Cerebral Blood Flow, and Cerebral Blood Volume

We modeled temporal response of CBF, CBV, and $CMRO_2$ with exponential rise and decay (29) as follows

$$\begin{aligned}&t < T_{on} : f(A, \tau, t) = 1\\ &T_{on} <= t <= T_{off} :\\ &\quad f(A, \tau, t) = A\{1 - \exp[-(t - T_{on})/\tau]\} + 1\\ &\quad t > T_{off} : f(A, \tau, t) = A\{1 - \exp[-(T_{off} - T_{on})/\tau]\}\\ &\quad \cdot \exp[-(t - T_{off})/\tau] + 1 \quad (4),\end{aligned}$$

where A is the maximum of the task-related increment compared with rest and τ is a time constant describing the increase or decrease after the onset and cessation of stimulation. Stimulation starts at T_{on} and ends at T_{off}. For simplicity, the time constants for the exponential rise and decay were set to equal τ.

From Equations [3] and [4], normalized total deoxyhemoglobin content per voxel is expressed as

$$\begin{aligned}\text{Normalized Total Deoxy-Hb (t)} &= f(A_{CMRO2}, \tau_{CMRO2}, t)\\ &\times f(A_{VBV}, \tau_{VBV}, t)/f(A_{CBF}, \tau_{CBF}, t) \quad (5)\end{aligned}$$

where A_{CMRO2} is maximum of the task-related increment of $CMRO_2$, A_{CBF} is that of CBF, and A_{VBV} is that of VBV and τ_{CMRO2}, τ_{CBF}, and τ_{VBV} are time constants for $CMRO_2$, CBF, and VBV, respectively.

Blood Oxygen Level-dependent Signal

Total Deoxy-Hb (t) was translated to a BOLD signal time course using an equation presented by Buxton et al. (17) as follows

$$\Delta S/S = V_0[k_1(1 - q) + K_2(1 - q/v) + k_3(1 - v)], \quad (6)$$

where ΔS is the BOLD signal change after stimulation, S is the BOLD signal at rest, V_0 is the venous blood volume fraction (%) at rest, q is the normalized total venous deoxyhemoglobin content during stimulation [q = Deoxy-Hb (act)/Deoxy-Hb (rest)], v is the normalized venous blood volume during stimulation ($v = V/V_0$), and V is the venous blood volume during stimulation. K_1, K_2, and K_3 are the constants depending on the static magnetic field (B_0), echo time (TE), OEF at rest (E_0), hematocrit (Ht), and the radius of the vessels (R) (31). Using this formula, we estimated that $K_1 = 3.5$, $K_2 = 2.2$, and $K_3 = 0.68$ for $B_0 = 1.5$ T, TE = 50 milliseconds, $E_0 = 0.4$, Ht = 40%, and R = 25 μm. We assumed that V_0 is 3%, because the total blood volume fraction in the cortical gray matter of the occipital lobe is 6% (32), half of which is occupied by capillary and arterial components (29,33).

Simulation

Using Equation 6, simulations were performed to investigate the effect of the increment of $CMRO_2$ on the task-related BOLD signal change, fixing the task-related change of CBF and CBV; A_{CBF}, A_{VBV}, τ_{CMRO2}, τ_{CBF}, and τ_{VBV} were held constant in the simulations. We assumed that the value of A_{CBF} was 60%. Previous positron emission tomography studies using 8 Hz of photic stimulation in adults revealed a more than 50% increase in CBF of the V1 (15). The value of A_{VBV} was set at 20% from the power law relation of $CBV = CBF^{0.38}$ (34). The value of τ_{VBV} was fixed at 20 seconds based on a previous report (29). Because task-related CBF response is more rapid than the CBV changes (29), we assumed the value of τ_{CBF} at 8 seconds. The task-related changes of CBF and CBV are shown in Figure 1. Although the detailed time course of task-related $CMRO_2$ change is not well known, the presence of the initial dip suggests that the task-related $CMRO_2$ response is more rapid than that of CBF (35–38). Hence, we set the value of τ_{CMRO2} shorter than that of CBF, that is, $\tau_{CMRO2} = 5$ seconds.

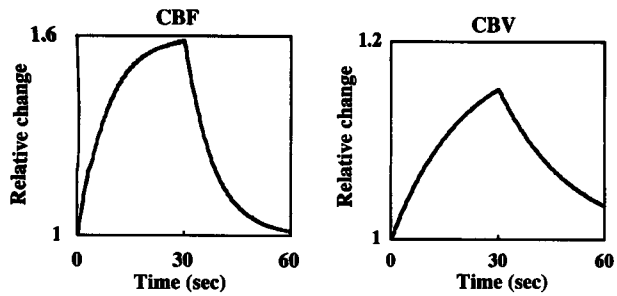

FIG. 1. Time courses of the simulated cerebral blood flow with a time constant of 8 seconds (**A**) and venous blood volume with a time constant of 20 seconds (**B**). The first 30 seconds is the task phase, followed by a rest phase of 30 seconds.

Fitting the Model to the Measured Data

Using Equation 6, we estimated A_{CMRO2} by fitting a theoretic BOLD signal time course to the measured data in each subject by the least-squares regression analysis. For this fitting, we used a total of 20 data points of the first stimulation phase and the following rest phase to eliminate the possible effect of the preceding hemodynamic changes in the following repeated phases. These time course data were converted to percentage of signal change from the average of the 10 time points in the first rest phase.

RESULTS

Infants and Adult Functional MRI

All infants showed a task-related signal change in the anterolateral region of the calcarine fissure. All infants in the younger infant group showed a task-related signal increase, and all members in the elder infant group showed a task-related signal decrease (see Table 1). The mean percentage of signal time course obtained from the younger infant group (Fig. 2A) showed a signal increase after the onset of stimulation, and the signal reached its peak after 15 seconds. The BOLD signal started decreasing at the cessation of stimulation, reached its lowest level 15 seconds later, and then returned to the baseline (poststimulus undershoot). The mean percentage of signal time course obtained from the elder infant group (see Fig. 2B) showed a signal decrease after the onset of stimulation, and the signal reached its lowest level after 12 seconds. After the cessation of stimulation, the BOLD signal increased and reached its peak over the baseline after 15 seconds; it then returned to the baseline level (poststimulus overshoot). The mean percentage of signal time course obtained from the adult group (see Fig. 2C) showed a signal increase after the onset of stimulation, and the signal reached its peak after 15 seconds. The BOLD signal started decreasing at the cessation of stimulation, reached its lowest level after 15 seconds, and then returned to the baseline level (poststimulus undershoot). The maximum change in mean BOLD signal time course was 1.21% ± 0.52% in the younger infant group, −1.91% ± 0.90% in the elder infant group, and 2.01% ± 0.63% in the adult group.

Simulation

Figure 3A shows the simulated time courses of $CMRO_2$, OEF, deoxyhemoglobin, and BOLD signals when A_{CMRO2} was set to 20% (A_{CMRO2}/A_{CBF} = 20/60 = 33.3%). In this setting, the BOLD signal time course showed a task-related signal increase. The BOLD signal increased by 2.7% at its peak. After the cessation of

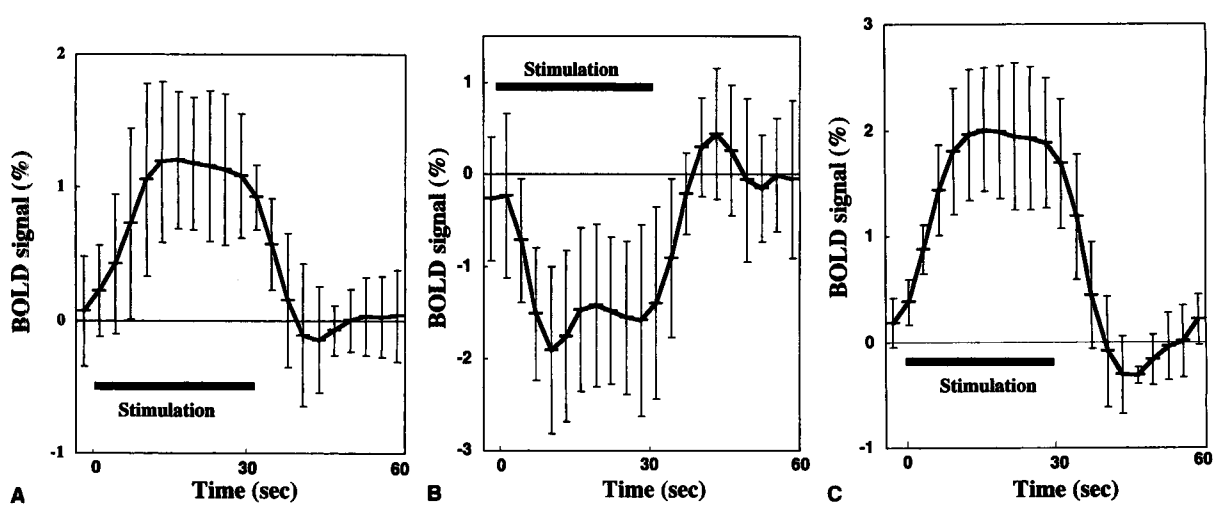

FIG. 2. Mean percentage of signal time courses of the visual cortex obtained from functional magnetic resonance imaging with photic stimulation in the younger infant group (<8 weeks of corrected age) (**A**), the elder infant group (>8 weeks of corrected age) (**B**), and adults (**C**). The first 30 seconds is the photic stimulation phase, followed by a rest phase of 30 seconds. A similar configuration of task-related blood oxygen level-dependent signal change is shared by younger infants and adults. Both show a task-related signal increment, followed by poststimulus undershoot. Conversely, the elder infant group shows a task-related decrement of the signal, followed by poststimulus overshoot.

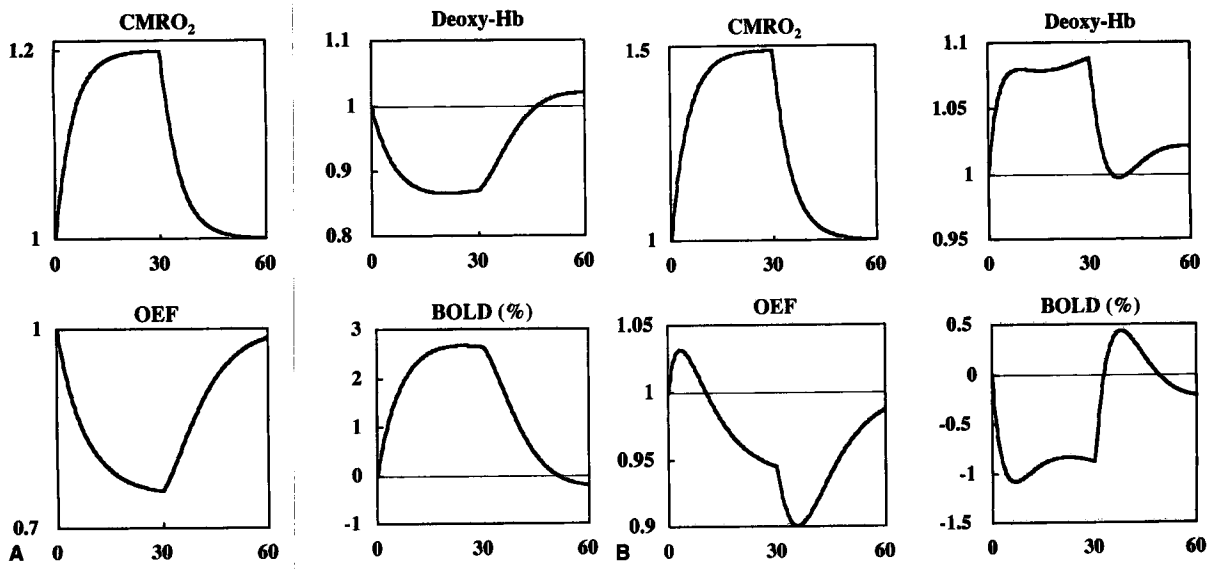

FIG. 3. (**A**) Time courses of the simulated cerebral metabolic rate of oxygen ($CMRO_2$) (upper left), oxygen extraction fraction (OEF) (lower left), total deoxyhemoglobin (upper right), and blood oxygen level-dependent (BOLD) signal (lower right) when the maximum task-related increment of $CMRO_2$ (A_{CMRO2}) is set to 20% and the time constant of $CMRO_2$ (τ_{CMRO2}) is 5 seconds. The BOLD signal showed a task-related increment. The first 30 seconds is the task phase, followed by a rest phase of 30 seconds. (**B**) The A_{CMRO2} is set to 50%. The BOLD signal shows a task-related decrement.

stimulation, the BOLD signal decreased under the baseline and showed a poststimulus undershoot.

Figure 3B shows the simulated time courses of $CMRO_2$, OEF, deoxyhemoglobin, and BOLD signals when A_{CMRO2} was set to 50% (A_{CMRO2}/A_{CBF} = 50/60 = 83%). In this setting, the BOLD signal time course showed a task-related signal decrease. After the onset of stimulation, the BOLD signal decreased and reached its lowest level. The BOLD signal decreased by 1.1% at its lowest level. After the cessation of stimulation, BOLD signal increased and peaked over the baseline. The OEF showed a transient increase during the early period of the stimulation phase followed by a decrease, reaching its lowest level after the cessation of stimulation. It was noted that the decrement of OEF decreased when the task-related increment of $CMRO_2$ increased.

Estimated Cerebral Metabolic Rate of Oxygen in Infants and Adults

The mean regression values were 0.70 ± 0.13 in the younger infant group, 0.78 ± 0.06 in the elder infant group, and 0.78 ± 0.18 in the adult group, indicating sufficient fitting. The mean values of the estimated A_{CMRO2} were 32.2% ± 4.7% in the younger infant group, 57.1% ± 8.8% in the elder infant group, and 26.3% ± 5.6% in the adult group. The plot of the estimated A_{CMRO2} against the corrected age (Fig. 4) indicates an abrupt increase in $CMRO_2$ at 8 weeks of age. The A_{CMRO2}/A_{CBF} was 0.53 ± 0.08 in the younger infant group, 0.95 ± 0.17 in the elder infant group, and 0.44 ± 0.09 in the adult group.

DISCUSSION

In the present simulation, we assumed that all the hemodynamic parameters except for the increment of $CMRO_2$ are constant across the three groups. An increase in BOLD signal as a result of photic stimulation has been observed in younger infants as well as in adults (20,24). The current study revealed that the configuration of task-related BOLD signal change in the younger infant group was similar to that in adults; hence, hemodynamic parameters may well be similar between younger

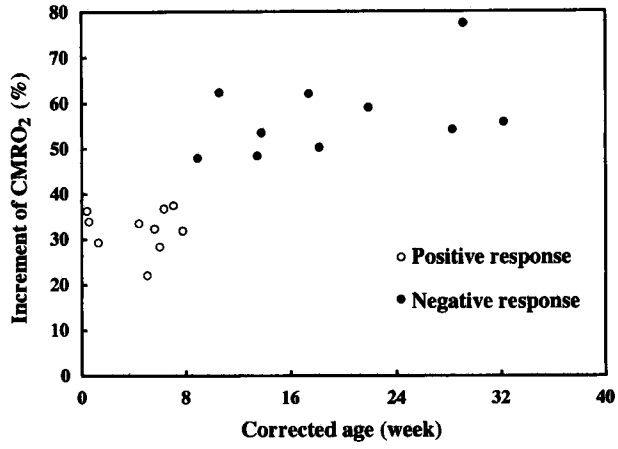

FIG. 4. The maximum task-related increments of the cerebral metabolic rate of oxygen (A_{CMRO2}) of the visual cortex of infants estimated from the blood oxygen level-dependent (BOLD) signal time course plotted against their corrected age. Open circles indicate that the BOLD response is positive, whereas the closed circles indicate a negative response.

infants and adults. It is unlikely that these parameters abruptly change at around 8 weeks of age.

The task-related signal change in the V1 in the younger infant group and in adults showed task-related increments of the signal followed by poststimulus undershoot. Mandeville et al. (29) measured the temporal change in CBV and BOLD signals in the rat brain and suggested that poststimulus undershoot originated from slow alteration of CBV, because the period of CBV delay temporally corresponded to the poststimulus undershoot. In accordance with this observation, the temporal change in CBV was set to 20 seconds (slower than that of CBF [8 seconds]) in our simulation, which replicated the poststimulus undershoot.

The elder infant group showed a task-related signal decrement followed by the poststimulus overshoot. Because the slower alteration of CBV than CBF reduces the poststimulus signal (17), this poststimulus overshoot should originate from another mechanism. Our simulation suggested that the difference between τ_{CMRO2} and τ_{CBF} created poststimulus overshoot, because the difference causes a transient poststimulus decrease in OEF, which temporally corresponded to poststimulus overshoot. This agreement of the BOLD signal time course in the simulation and experimental study supports our assumption of the shorter time constant of $CMRO_2$ (5 seconds) than that of CBF (8 seconds). These results confirm the feasibility of the parameter settings of our simulation.

The present study demonstrated that a large task-related increment of $CMRO_2$ (A_{CMRO2}) reverses the signal response pattern in fMRI when all other parameters are fixed. This result suggests that change in A_{CMRO2}/A_{CBF} is a determinant of the BOLD signal change. A_{CMRO2} and A_{CMRO2}/A_{CBF} during photic stimulation of the V1 have been measured using positron emission tomography and MRI ranging widely from 5% to 30% and from 0.1 to 0.7, respectively (15,39–41). The mean A_{CMRO2} and A_{CMRO2}/A_{CBF} in normal adults in this study were 26% and 0.44, respectively, which is consistent with the results noted in most previous reports. Thus, our BOLD signal model can be considered appropriate for estimation of the increment of $CMRO_2$.

The mean estimated A_{CMRO2} in the elder infant group (57.1% ± 8.8%) was twice as large as that of the younger infant group (32.2% ± 4.7%). Because the metabolic activity of the synapse determines the net aerobic metabolism of the cerebral cortex (1), $CMRO_2$ increase during activation is expected to be proportional to synaptic density. The synaptic density of the V1 in the term newborn increases by more than two times by several months and peaks at about twice the level of adults (21,22). Considering that the most of the energy metabolism (i.e., oxygen consumption and glucose utilization) and its task-related changes occur at the synapse level (1), an abrupt increase in estimated A_{CMRO2}/A_{CBF} at around 8 weeks may represent an increase in synaptic density. In other words, the reversal of the task-related BOLD signal change from positive to negative at 8 weeks of age indicates rapid synaptogenesis.

CONCLUSIONS

We applied the mathematic model of BOLD signal change, which is based on human adult and animal experiments, to infant data. The simulations demonstrated that the task-related BOLD signal change undergoes a positive to negative conversion, as indicated by the change in the increment of $CMRO_2$. The mean estimated $CMRO_2$ of the V1 in the elder infant group during photic stimulation was twice as large as that of the younger group. Hence, a change of oxygen consumption with age can explain a transition from a positive to a negative BOLD response. A change of oxygen consumption is parallel to changes in synaptic density. Because the timing of the reversal of the task-related BOLD signal change corresponded to that of rapid synaptogenesis in V1, the biphasic change represents dynamic synaptogenesis in the V1 at approximately 8 weeks.

Acknowledgment: This study was in part supported by a research grant (JSPS-RFTF97L00203) from the Japan Society for the Promotion of Science.

REFERENCES

1. Raichle ME. Circulatory and metabolic correlates of brain function in normal humans. In: Mountcastle VB, Plum F, Geiger SR, eds. *Handbook of physiology*. New York: Oxford University Press, 1987:643–74.
2. Edelman RR, Siewert B, Darby DG, et al. Qualitative mapping of cerebral blood flow and functional localization with echo-planar MR imaging and signal targeting with alternating radio frequency. *Radiology* 1994;192:513–20.
3. Connelly A, Dettmers C, Stephan KM, et al. Quantitative comparison of functional magnetic resonance imaging and positron emission tomography using a controlled-force motor paradigm. In: Proceedings of the Society of Magnetic Resonance Third Annual Meeting, Nice, 1995:786.
4. Kim SG. Quantification of relative cerebral blood flow change by flow-sensitive alternating inversion recovery (FAIR) technique: application to functional mapping. *Magn Reson Med* 1995;34:293–301.
5. Ramsey NF, Kirkby BS, Van Gelderen P, et al. Functional mapping of human sensorimotor cortex with 3D BOLD fMRI correlates highly with H2(15)O PET rCBF. *J Cereb Blood Flow Metab* 1996;16:755–64.
6. Zhu XH, Kim SG, Andersen P, et al. Simultaneous oxygenation and perfusion imaging study of functional activity in primary visual cortex at different visual stimulation frequency: quantitative correlation between BOLD and CBF changes. *Magn Reson Med* 1998;40:703–11.
7. Silva AC, Lee SP, Yang G, et al. Simultaneous blood oxygenation level-dependent and cerebral blood flow functional magnetic resonance imaging during forepaw stimulation in the rat. *J Cereb Blood Flow Metab* 1999;19:871–9.
8. Ogawa S, Lee TM, Kay AR, et al. Brain magnetic resonance imaging with contrast dependent on blood oxygenation. *Proc Natl Acad Sci USA* 1990;87:9868–72.
9. Belliveau JW, Rosen BR, Kantor HL, et al. Functional cerebral imaging by susceptibility-contrast NMR. *Magn Reson Med* 1990; 14:538–46.

10. Bandettini PA, Wong EC, Hinks RS, et al. Time course EPI of human brain function during task activation. *Magn Reson Med* 1992;25:390–7.
11. Kwong KK, Belliveau JW, Chesler DA, et al. Dynamic magnetic resonance imaging of human brain activity during primary sensory stimulation. *Proc Natl Acad Sci USA* 1992;89:5675–9.
12. Pauling L, Coryell CD. The magnetic properties of and structure of hemoglobin, oxyhemoglobin and carbonmonoxyhemoglobin. *Proc Natl Acad Sci USA* 1936;22:210–6.
13. Buxton RB, Frank LR. A model for the coupling between cerebral blood flow and oxygen metabolism during neural stimulation. *J Cereb Blood Flow Metab* 1997;17:64–72.
14. Fox PT, Raichle ME. Focal physiological uncoupling of cerebral blood flow and oxidative metabolism during somatosensory stimulation in human subjects. *Proc Natl Acad Sci USA* 1986;83: 1140–4.
15. Fox PT, Raichle ME, Mintun MA, et al. Nonoxidative glucose consumption during focal physiologic neural activity. *Science* 1988;241:462–4.
16. Ogawa S, Tank DW, Menon R, et al. Intrinsic signal changes accompanying sensory stimulation: functional brain mapping with magnetic resonance imaging. *Proc Natl Acad Sci USA* 1992;89: 5951–5.
17. Buxton RB, Wong EC, Frank LR. Dynamics of blood flow and oxygenation changes during brain activation: the balloon model. *Magn Reson Med* 1998;39:855–64.
18. Born P, Rostrup E, Leth H, et al. Change of visually induced cortical activation patterns during development [letter]. *Lancet* 1996;347:543.
19. Yamada H, Sadato N, Konishi Y, et al. A rapid brain metabolic change in infants detected by fMRI. *Neuroreport* 1997;8:3775–8.
20. Yamada H, Sadato N, Konishi Y, et al. A milestone for normal development of the infantile brain detected by functional MRI. *Neurology* 2000;55:218–23.
21. Huttenlocher PR, de Courten C, Garey LJ, et al. Synaptogenesis in human visual cortex—evidence for synapse elimination during normal development. *Neurosci Lett* 1982;33:247–52.
22. Huttenlocher PR, de Courten C. The development of synapses in striate cortex of man. *Hum Neurobiol* 1987;6:1–9.
23. Chugani HT, Phelps ME. Maturational changes in cerebral function in infants determined by 18FDG positron emission tomography. *Science* 1986;231:840–3.
24. Morita T, Kochiyama T, Yamada H, et al. Difference in the metabolic response to photic stimulation of the lateral geniculate nucleus and the primary visual cortex of infants: a fMRI study. *Neurosci Res* 2000;38:63–70.
25. Friston KJ, Worsley KJ, Frackowiak RSJ, et al. Assessing the significance of focal activations using their spatial extent. *Hum Brain Map* 1994;1:210–20.
26. Friston KJ, Holmes AP, Poline JB, et al. Analysis of fMRI time-series revisited. *Neuroimage* 1995;2:45–53.
27. Born P, Leth H, Miranda MJ, et al. Visual activation in infants and young children studied by functional magnetic resonance imaging. *Pediatr Res* 1998;44:578–83.
28. Martin E, Joeri P, Loenneker T, et al. Visual processing in infants and children studied using functional MRI. *Pediatr Res* 1999;46: 135–40.
29. Mandeville JB, Marota JJ, Kosofsky BE, et al. Dynamic functional imaging of relative cerebral blood volume during rat forepaw stimulation. *Magn Reson Med* 1998;39:615–24.
30. Hathout GM, Varjavand B, Gopi RK. The early response in fMRI: a modeling approach. *Magn Reson Med* 1999;41:550–4.
31. Boxerman JL, Bandettini PA, Kwong KK, et al. The intravascular contribution to fMRI signal change: Monte Carlo modeling and diffusion-weighted studies in vivo. *Magn Reson Med* 1995;34: 4–10.
32. Leenders KL, Perani D, Lammertsma AA, et al. Cerebral blood flow, blood volume and oxygen utilization. Normal values and effect of age. *Brain* 1990;113:27–47.
33. Pawlik G, Rackl A, Bing RJ. Quantitative capillary topography and blood flow in the cerebral cortex of cats: an in vivo microscopic study. *Brain Res* 1981;208:35–58.
34. Grubb RL, Jr, Raichle ME, Eichling JO, et al. The effects of changes in PaCO2 on cerebral blood volume, blood flow, and vascular mean transit time. *Stroke* 1974;5:630–9.
35. Ernst T, Hennig J. Observation of a fast response in functional MR. *Magn Reson Med* 1994;32:146–9.
36. Menon RS, Ogawa S, Hu X, et al. BOLD based functional MRI at 4 Tesla includes a capillary bed contribution: echo-planar imaging correlates with previous optical imaging using intrinsic signals. *Magn Reson Med* 1995;33:453–9.
37. Malonek D, Grinvald A. Interactions between electrical activity and cortical microcirculation revealed by imaging spectroscopy: implications for functional brain mapping. *Science* 1996;272: 551–4.
38. Hu X, Le TH, Ugurbil K. Evaluation of the early response in fMRI in individual subjects using short stimulus duration. *Magn Reson Med* 1997;37:877–84.
39. Marret S, Gjedde A. Changes of blood flow and oxygen consumption in visual cortex of living humans. *Adv Exp Med Biol* 1997; 413:205–8.
40. Davis TL, Kwong KK, Weisskoff RM, et al. Calibrated functional MRI: mapping the dynamics of oxidative metabolism. *Proc Natl Acad Sci USA* 1998;95:1834–9.
41. Hoge RD, Atkinson J, Gill B, et al. Investigation of BOLD signal dependence on cerebral blood flow and oxygen consumption: the deoxyhemoglobin dilution model. *Magn Reson Med* 1999;42: 849–63.